Received: 15 February 2021 | Revised: 5 April 2021 | Accepted: 7 April 2021

DOI: 10.1002/aoc.6271

FULL PAPER

Applied Organometallic Chemistry WILEY

Ultrasonic-assisted preparation of Co_3O_4 and Eu-doped Co_3O_4 nanocatalysts and their application for solvent-free synthesis of 2-amino-4*H*-benzochromenes under microwave irradiation

Leila Kafi-Ahmadi[1] | **Ahmad Poursattar Marjani**[2] | **Ehsan Nozad**[2]

[1]Department of Inorganic Chemistry, Faculty of Chemistry, Urmia University, Urmia, Iran

[2]Department of Organic Chemistry, Faculty of Chemistry, Urmia University, Urmia, Iran

Correspondence
Ahmad Poursattar Marjani, Department of Organic Chemistry, Faculty of Chemistry, Urmia University, Urmia, Iran.
Email: a.poursattar@urmia.ac.ir; a.poursattar@gmail.com

Funding information
Urmia University

Co_3O_4 and Eu-doped Co_3O_4 nanocatalysts were synthesized through an ultrasonic-assisted solvothermal method and were characterized with X-ray diffraction (XRD), Fourier transform infrared (FT-IR), energy-dispersive X-ray (EDX), and field-emission scanning electron microscopy (FESEM) methods. Spinel cubic crystalline system for synthesized nanocatalysts was confirmed with XRD, whereas the spherical morphology of Co_3O_4 changed to nanorods after Eu^{3+} doping, which was affirmed with FESEM micrographs. Catalytic performance of the nanomaterials was examined through the synthesis of 2-amino-4*H*-benzochromenes using aromatic aldehydes, malononitrile, and β-naphthol condensation under solvent-free conditions and microwave irradiation. Mild reaction conditions, short reaction times, simple setup, using an affordable catalyst, and high-quality products were some of the advantages of this procedure. The efficiency for Eu-doped nanocatalyst was achieved by about 96%.

KEYWORDS

2-amino-4*H*-benzochromenes, Co_3O_4, Eu-doped Co_3O_4, nanocatalyst, solvent-free synthesis

1 | INTRODUCTION

2-Amino-4*H*-benzochromene derivatives are outstanding categories of oxygen heterocyclic chemicals having a broad spectrum of interesting pharmacological and biological attributes, for instance, cytotoxic, antitumor, antiproliferative, and antibacterial characteristics.[1–5] Besides, cosmetics, pigments, and being parts of numerous natural products are the other plus points of these products. Therefore, the development of an efficient and suitable methodology to synthesize these compounds is profoundly imperative.[6–10] Some diverse 2-amino-4*H*-bezochromenes with strong pharmacological properties are indicated in Figure 1.

The simplest synthesized procedure includes a three-component cyclocondensation reaction of aromatic aldehydes, malononitrile (as a nucleophile), and various enolizable C–H activated compounds. However, some organic solvent sources used in an aforementioned procedure such as piperidine, pyridine, and triethylamine may cause to several hours of reaction time.[11] Moreover, other catalysts including methanesulfonic acid, imidazole, porous organic polymers (POPs), potassium phthalimide, L-proline–melamine, sodium malonate, and Na_2CO_3 have been utilized for this transformation. Recently, several novel green approaches have been reported using cetyltrimethylammonium chloride (CTAC), KF/Al_2O_3, basic γ-alumina, MgO, $CuSO_4{\cdot}5H_2O$,

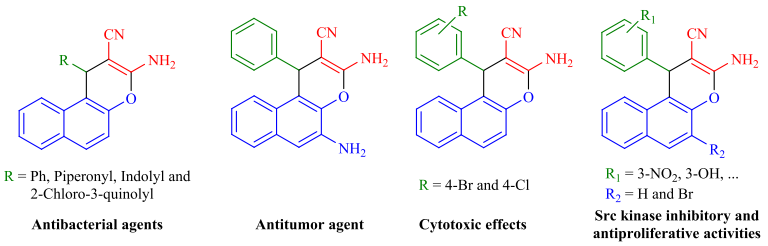

FIGURE 1 Representative examples of 2-amino-4*H*-benzochromene moieties with biological virtues

1,8-diazabicyclo[5.4.0]undec-7-ene (DBU), CTABr/ultrasound irradiation, nanocatalyst, bael fruit extract, water extract of lemon fruit shell ash, and poly(ethylene glycol) (PEG) in water.[12–26]

One-pot, multicomponent reactions (MCRs) are widely used and an approved method due to their atom economy, high efficiency, and selective bond formations for synthesizing different types of heterocyclic compounds such as benzochromens, benzopyrans, and so many other materials with various applications.[27–37]

Microwave irradiation is a novel and practical technique for reagent activation in synthesis of the organic compounds. This method has been applied successfully for the synthesis of heterocyclic compounds under moderate conditions, which have gained its popularity through the less reaction duration, modified products, environmental and commercial advantages, and simplified setup in comparison with conventional heating reactions.[38,39]

Among the metallic oxides, components including spinel-type tricobalt tetraoxide (Co_3O_4) have drawn profound attention in as much as a pivotal role in Li-ion rechargeable batteries, antiferromagnetic p-type semiconductor, magnetic materials, and electrochemical devices. Currently, several methods (i.e., hydrothermal, sol–gel, chemical spray pyrolysis [CSP], microemulsion, chemical vapor deposition [CVD], thermal decomposition of cobalt precursors, sonochemical route, microwave irradiation, coprecipitation, and mechanochemical processing) are used for the synthesis of Co_3O_4. Although various morphologies of nanostructured Co_3O_4 have been synthesized, the producing orders need either challenging technique or severe conditions.[40–43] For instance, Salehi et al. synthesized Co_3O_4, $Co_{3-x}NdxO_4$, and $Co_{3-x}EuxO_4$ nanoparticles by combustion synthesis method at the temperature of 700°C for 8 h. Co_3O_4 nanoparticle had cubic shape with spherical particles a few void numbers on the surface but in the $Co_{3-x}NdxO_4$ and $Co_{3-x}EuxO_4$, the particles had homogeneous structure.[44]

The aim of this study is the synthesis of Co_3O_4 (S_1) and Eu-doped Co_3O_4 (S_2) nanostructures by ultrasonic-assisted solvothermal procedure as a novel and cost-effective method. Characterization was conducted by Fourier transform infrared (FT-IR) and X-ray powder diffraction (PXRD) techniques. The morphology of products was evaluated using field-emission scanning electron microscopy (FESEM). The efficiency of the synthesized nanocatalysts was investigated as efficient recyclable catalysts for the synthesis of 2-amino-4*H*-benzochromenes under solvent-free conditions and microwave irradiation (Scheme 1).

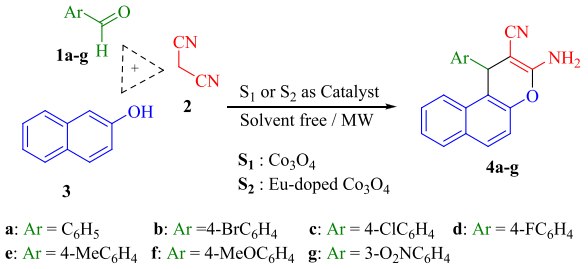

SCHEME 1 The synthetic pathway of 2-amino-4*H*-benzochromene derivatives. MW, molecular weight

2 | EXPERIMENTAL

2.1 | Materials and methods

All precursors for the synthesis were purchased from Merck (Germany), and no excess purification was carried out. PXRD patterns of the samples were recorded by a D5000 powder X-ray diffractometer (Siemens AG, Munich, Germany) using Cu Kα radiation. FT-IR spectra were provided using KBr pellets on a "Bruker Tensor" instrument. The morphology of the products was evaluated through a field-emission scanning electron microscope (Hitachi FESEM, Mo. S-4160). Melting points were determined using a finely powdered sample in a fused capillary with a melting point apparatus (Elico). Microwave-assisted procedures were performed at 1600 W in the Milestone microwave oven. Both ^{1}H-NMR at 400 MHz and ^{13}C-NMR at 100-MHz spectra were achieved with a Bruker Avance AQS 400 MHz, ultrashield in DMSO-d_6 as a solvent and Me_4Si as an internal reference, and the chemical shifts are represented by units of ppm. Mass spectra of the all compounds were recorded using LCMS-2010A, Shimadzu. Elemental compositions of the nanocatalysts were investigated using energy-dispersive X-ray (EDX) spectroscopy.

2.2 | Synthesis

2.2.1 | Synthesis of Co_3O_4 (S_1)

A total of 2.0 mM (582 mg) of $Co(NO_3)_2{\cdot}6H_2O$ (molecular weight [MW] = 291.03 g mol^{-1}) was dissolved in 10 ml of distilled water. Then, 20 ml of EtOH was added to the prepared mixture under stirring for 15 min at 60°C. Afterward, a 4-M solution of KOH was used to adjust the mixture pH at 12 and was stirred for 15 min and kept under ultrasonic agitation for 30 min at room temperature. A 60-ml Teflon-lined stainless steel sealed autoclave was used to heat the solution. The heating process was continued until reaching up to 180°C temperature for 8 h. After reaction completion, the autoclave was cooled down by water to the room temperature. The achieved powders were rinsed by distilled water and dried at 90°C for 5 h in the room ambient (yield = 81%).

2.2.2 | Synthesis of $Co_{2.97}Eu_{0.03}O_4$ (S_2)

A total of 2.97 mM (864 mg) of $Co(NO_3)_2{\cdot}6H_2O$ (MW = 291.03 g mol^{-1}) and 0.03 mM (11 mg) of Eu_2O_3 (MW = 351.92 g mol^{-1}) were added to 10 ml of H_2O. Next, 20 ml of ethanol was added to the solution and was stirred for 15 min at 60°C. The same steps of reaction were accomplished to the synthesis of the Co_3O_4 (yield = 89%).

2.2.3 | General procedure for the synthesis of 2-amino-4*H*-benzochromene with diverse substituents 4a–g

Substituted aromatic aldehydes (1 mmol), malononitrile (1 mmol), β-naphthol (1 mmol), and S_1 nanoparticles (30 mg) were all mixed in a flask (50 ml) and irradiated with microwave (500 W). The end of the reaction was investigated with thin-layer chromatography (TLC) analysis (hexane:ethylacetate/6:4). Upon reaction completion, the resulting product was heated in ethanol. The catalyst was separated by filtration from the mixture and rinsed several times with aqueous ethanol for reuse. Then, the residue was added to crushed ice and was stirred for a couple of minutes. The compact product was filtered off by suction and recrystallized from aqueous ethanol to collect the desired 2-amino-4*H*-benzochromenes in high yields. The successful synthesize of the 2-amino-4H-benzochromenes was affirmed using 1H-NMR and 13C-NMR analysis. (see supplementary information)

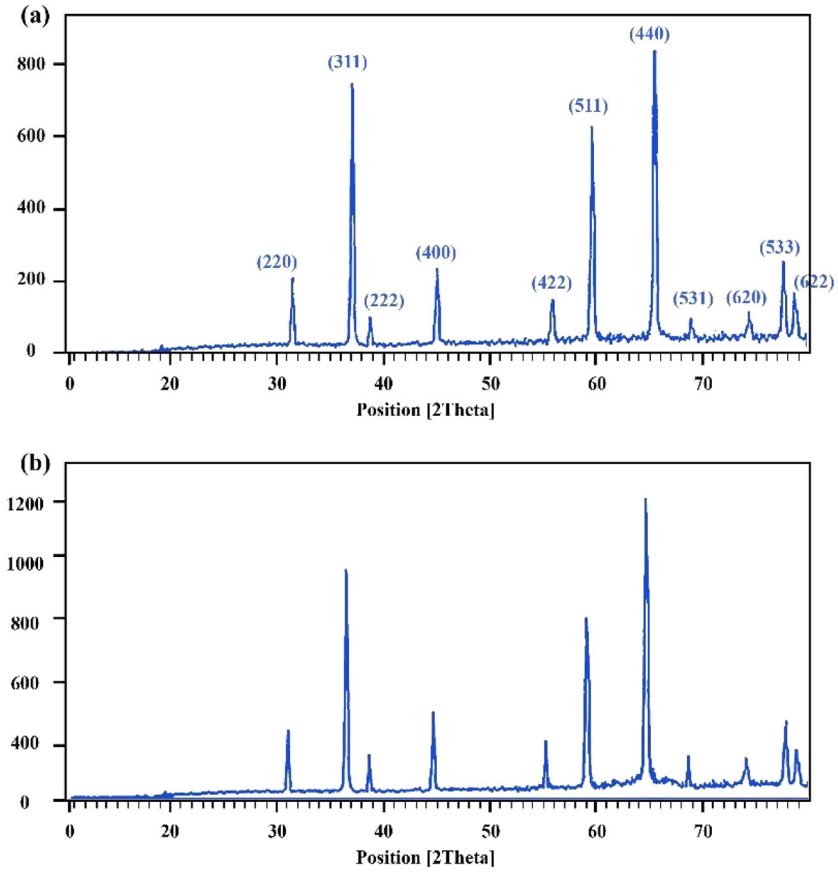

FIGURE 2 X-ray diffraction (XRD) spectrum of (a) S_1 and (b) S_2

3 | RESULTS AND DISCUSSIONS

3.1 | X-ray diffraction analysis

The crystallographic information of both samples (S_1 and S_2) was gathered with PXRD. Figure 2a, presents the PXRD pattern of the S_1 nanoparticles prepared through the solvothermal method. Diffraction lines are assigned to the reflections 220°, 311°, 222°, 400°, 422°, 511°, 440°, 531°, 620°, 533°, and 622°, respectively, which correspond to the spinel cubic structure of Co_3O_4 with Fd3m space group with lattice parameters of cubic structure $a = b = c = 8.081$ Å. No peaks of other phases or impurities were detected, indicating the high purity of the Co_3O_4 product. (JCPDS Card No. 43-1003).[45]

Figure 2b, displays the XRD patterns of S_2. There are no additional XRD lines attributed to the secondary phase; hence, it is evident that Co^{3+} is replaced by Eu^{3+}. Table 1, manifests the cell parameter refinement data for the pure and doped nanomaterial. It can be seen that the cubic structure is not altered by doping, whereas the changes in the intensity of the peaks exhibit that the crystallinity is affected because of accomplished doping. Besides, there is a marginal shift in the position of the doped sample peak owing to the changes in lattice constants. According to the Scherrer equation, $D = 0.9\lambda/\beta\cos\theta$, whereas D is the average crystallite size, λ is the X-ray wavelength, θ is the angle of diffraction, and β is the full width at half maximum of the most intense peak. The average size of nanoparticles was calculated as outlined in Table 1.

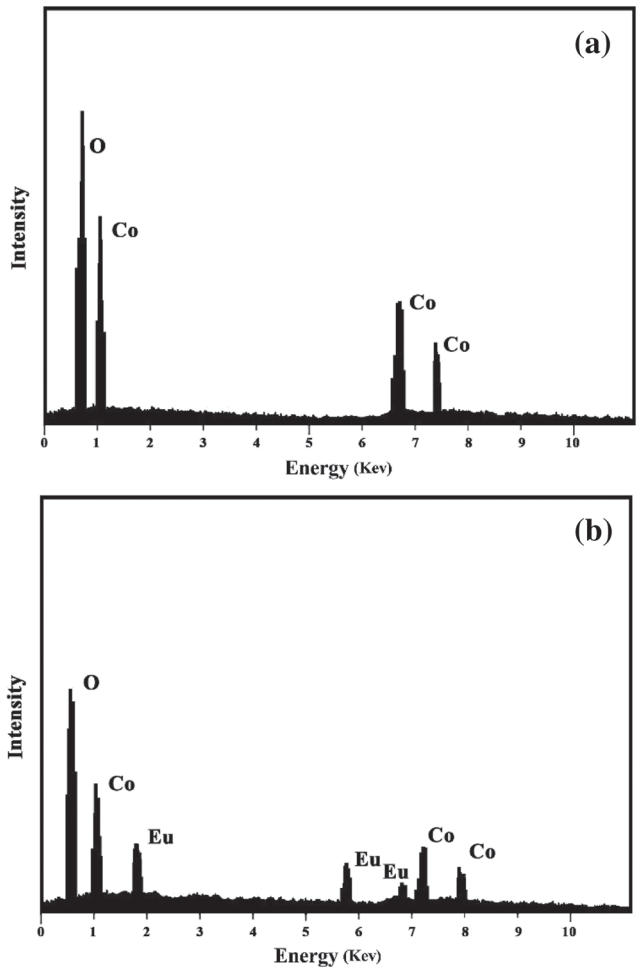

FIGURE 3 Energy-dispersive X-ray (EDX) spectra of (a) Co_3O_4 and (b) Eu-dopped Co_3O_4

3.2 | Elemental analysis

The compositions of the synthesized nanocatalyst before and after doping Eu were studied qualitatively through EDX analysis. The patterns are exhibited in Figure 3. As can be observed in Figure 3a, the spectrum confirms the pure composition of Co_3O_4 which is composed of Co and O only. On the other hand, Eu-doped nanocatalyst spectrum (Figure 3b) clearly shows the appeared Eu-associated peaks; moreover, a decrease in intensity of the Co peaks affirms the triumphantly doped Eu within the Co_3O_4 structure instead of Cobalt nondestructively.

TABLE 1 Average nanocrystal size and cell parameter refinement data for the samples

Sample	Crystallite size (nm)	$a = b = c$ (Å)
Co_3O_4	30	8.081
$Co_{2.97}Eu_{0.03}O_4$	27	8.079

3.3 | Morphology

FESEM images were observed to determine the morphology of nanomaterials. Figure 4a, illustrates the FESEM images of spinel Co_3O_4. As can be seen in Figure 4a,b, S_1 has compact agglomerated spherical nanocrystals, whereas Eu^{3+} doped into Co_3O_4 (S_2) resulted in nanorod-shaped crystals. Therefore, the product consists of rods with various lengths and thicknesses.

3.4 | N_2-physical adsorption measurement

The physical feature of nanomaterials was taken into account to gain in-depth insight. In this respect, the surface area of the nanocatalyst, its average pore size, and also the average pore volume of the synthesized powders were characterized. Before conducting the measurement, the samples were degreased for 2 h at 150°C in a nitrogen

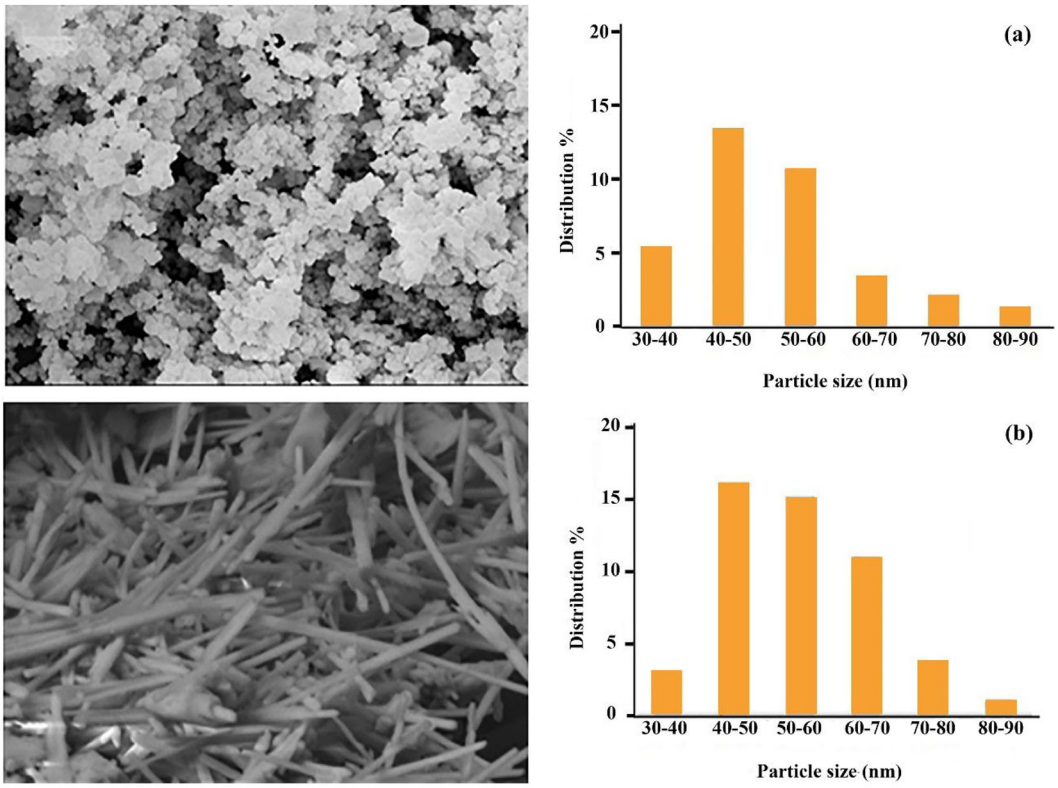

FIGURE 4 Field-emission scanning electron microscopy (FESEM) micrographs of (a) S_1 and (b) S_2 samples

TABLE 2 Structural properties of the catalysts

Sample	S_{BET} ($m^2\ g^{-1}$)	Pore volume ($cm^3\ g^{-1}$)	Pore diameter (nm)
S_1	3.246	0.0154	18
S_2	4.770	0.1340	23

bath. Next, the specific surface area (S_{BET}) of the samples was calculated using the isotherms at 77 K (−196°C). The measured physical features of the samples are shown in Table 2. The average surface areas were approximately 3.246 and 4.770 $m^2\ g^{-1}$, though pore volumes were about 0.0154 and 0.1340 $cm^3\ g^{-1}$ for S_1 and S_2, respectively. As can be interpreted, doping of Eu^{3+} to Co_3O_4 leads to the expansion of the surface area, pore volume, and the average pore diameter of the catalyst, simultaneously.

Table 3, depicts the textural properties of S_1 and S_2 according to the Barrett–Joyner–Halenda (BJH) method, which reveals that the S_{BET} of the pores, pore width, and volume of S_1 are smaller than those of S_2. Moreover, the BET results and BJH measurements claim that the surface area, average pore diameter sizes, and the average pore volume of S_1 are smaller than those of S_2.

TABLE 3 BJH data for S_1 and S_2 and the textural properties of the products

BJH desorption property	Value	
	S_1	S_2
Cumulative surface region of pores between 17- and 3000-Å width	4.120	5.581
Cumulative volume of pores between 17- and 3000-Å width	0.0159	0.1347
Average pore width (4 V A^{-1})	17	24

Abbreviation: BJH, Barrett–Joyner–Halenda.

3.5 | FT-IR spectroscopy

Figure 5, illustrates the FT-IR spectra of S_1 and S_2 nanocrystals. In the studied domain (4000–400 cm^{-1}), the obtained spectra indicate portions of two absorption bands at 574 υ_1) and 667 (υ_2) cm^{-1} for S_1, plus 579 υ_1) and 677 υ_2) cm^{-1} for S_2, in a row. These absorptions are signs of metal–oxygen stretching vibrations and prove the Co_3O_4 spinel oxide formations. The υ_1 and υ_2 bands are associated with OB_3 and ABO_3 vibrations in the spinel lattice, respectively, whereas B and A represent the Co^{3+} in the octahedral and tetrahedral holes accordingly.[46]

3.6 | Application of the prepared nanocatalysts for the synthesis of 2-amino-4*H*-benzochromenes

The activity of the synthesized catalysts for preparing the 2-amino-4*H*-benzochromene derivatives was investigated.

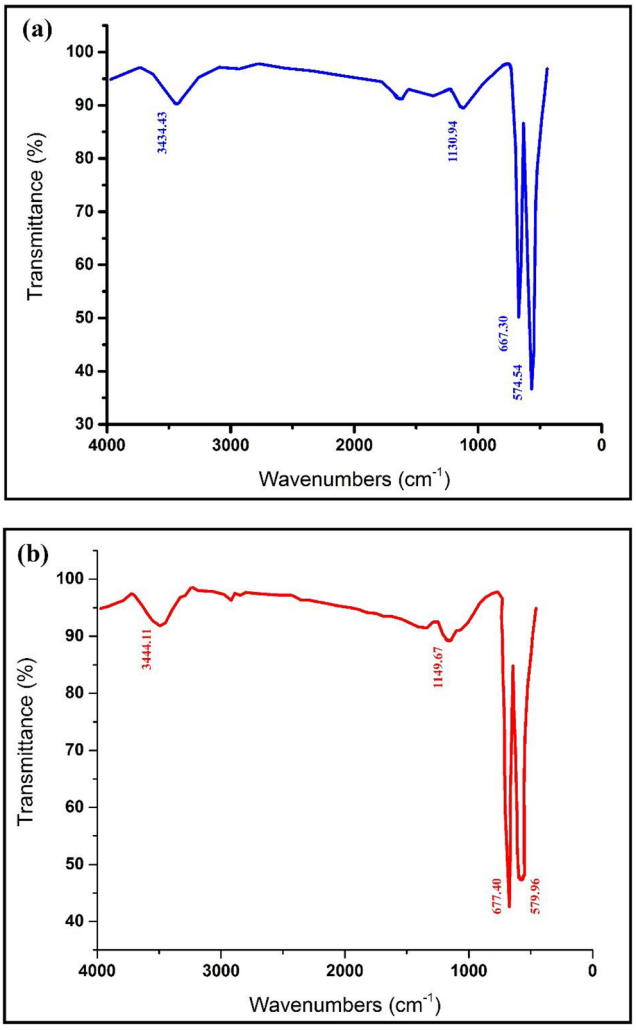

FIGURE 5 Fourier transform infrared (FT-IR) spectra of (a) S_1 and (b) S_2

The one-pot, three-component reaction (TCR) of benzaldehyde, malononitrile, and β-naphthol in a catalytic amount of S_1 was regarded as a norm. Several conditions have been studied in a pilot experiment, concerning optimum conditions. Then, the evaluation of the scope and constraints of the reaction was accomplished using various substituted aryl aldehydes as substrate compounds. Therefore, the catalytic applicability of the S_1 was reviewed for providing the target molecule. The reaction was carried out by different amounts of S_1 under solvent-free conditions (Table 4). As indicated in Table 4, entry 4, excellent results were achieved using 30 mg of nanocatalyst when no solvent was used. Moreover, an increase in catalyst amount had no significant effect on the outcome. Furthermore, no progress in the reaction was monitored in the absence of a nanocatalyst.

The effect of various solvents on a model reaction was investigated (Table 5). EtOH, H_2O, EtOH/H_2O (1:1), CH_2Cl_2, CH_3CN, and *n*-hexane were used for this purpose. Nevertheless, no significant reaction progress was monitored even after the prolonged span. As shown in Table 4, in the solvent-free condition, the yield of the reaction was quite satisfying (94%).

Table 6, presents the catalytic performance of S_1 and S_2 under the optimum conditions using multiple raw material derivatives. As an outcome, electron-donating

TABLE 5 Optimization of solvent in the synthesis of 2-amino-4*H*-benzochromene under 500 W

Entry	Solvent	Yield[a] (%)
1	—	94
2	H_2O	72
3	EtOH	56
4	EtOH/H_2O (1:1)	66
5	CH_2Cl_2	Trace
6	CH_3CN	—
7	*n*-Hexane	Trace

[a]Yield of isolated products.

TABLE 4 Catalyst amount optimization in the synthesis of 2-amino-4*H*-benzochromene[a] at 500 W

Entry	Amount of catalyst (mg), S_1	Time (min)	Yield[b] (%)
1	—	4	—
2	10	4	63
3	20	4	77
4	30	4	94
5	40	4	94
6	50	4	94

[a]Reaction was performed with benzaldehyde (1 mM), malononitrile (1 mM), β-naphthol (1 mM), and catalyst.
[b]Isolated yield.

TABLE 6 Synthesis of 2-amino-4*H*-benzochromenes catalyzed by S_1 or S_2 nanocatalysts

Entry	Aldehyde	Products	Yield[a] (%) S_1	Time (min)	Yield[a] (%) S_2	Time (min)	m.p.[b] (°C) Obsd.	m.p.[b] (°C) Lit.
1	C_6H_5CHO	**4a**	94	4	96	6	286–287	285–287[47]
2	$4\text{-}BrC_6H_4CHO$	**4b**	95	6	97	6	218–220	220–222[7]
3	$4\text{-}ClC_6H_4CHO$	**4c**	95	5	97	4	205–208	210–212[48]
4	$4\text{-}FC_6H_4CHO$	**4d**	96	5	97	4	236–238	239–241[7]
5	$4\text{-}MeC_6H_4CHO$	**4e**	88	4	89	7	269–271	269–271[49]
6	$4\text{-}MeOC_6H_4CHO$	**4f**	87	7	89	5	189–190	191–193[7]
7	$3\text{-}O_2NC_6H_4CHO$	**4g**	97	7	98	6	232–234	232–235[50]

[a]Yield refers to isolated pure products.
[b]Products were characterized by comparison of melting points of the known products reported in the literature.

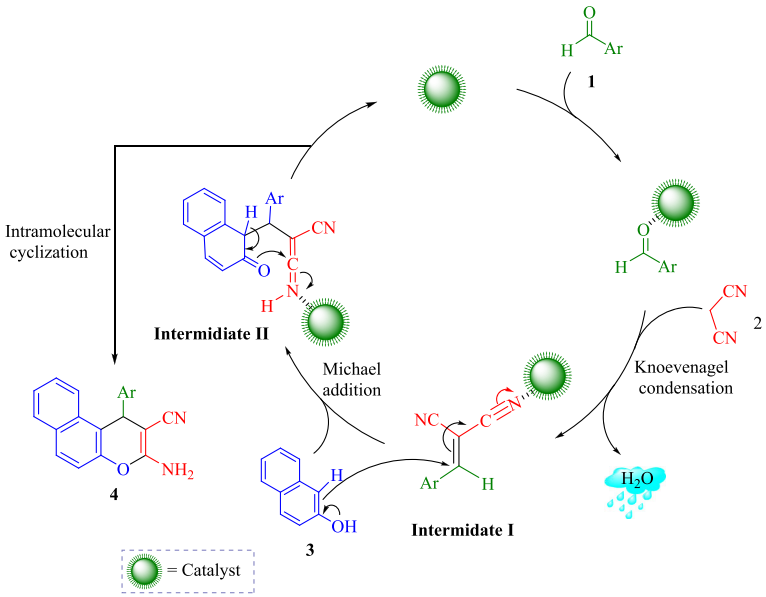

SCHEME 2 Suggested mechanism for the synthesis of 2-amino-4*H*-benzochromenes catalyzed by S_1 or S_2

groups on the aromatic aldehyde rings result in low yields of the corresponding products, and the reaction was slow, whereas electron-withdrawing groups result in higher amounts of yield. After completion of the reaction, the catalysts were readily removed by filtration, and the products were filtered out after solvent evaporation and easily purified by recrystallization from ethanol.

Scheme 2, exhibits the probable mechanism of reaction for the synthesis 2-amino-4*H*-benzochromenes by TCR, catalyzed by S_1/S_2 under solvent-free conditions. The reaction gets initiated by the activation of aldehyde between the nanocatalyst and the oxygen of the carbonyl group in the aromatic aldehyde. Simultaneously, the Knoevenagel condensation takes place between activated aromatic aldehydes **1** with malononitrile (**2**) by the loss of one molecule of water to generate intermediate **I**. After that, the Michael-type addition of β-naphthol (**3**) to intermediate **I** to give intermediate **II**, which goes for intramolecular heterocyclization by the nucleophilic attack of oxygen atom to C═N group of intermediate **II**, leads to form in situ the desired products **4**. In the path of mechanism, catalyst plays a pivotal role in accelerating all steps of the reaction and is regenerated at the end of the cycle.

The catalytic performance comparison of S_1 and S_2 under the optimum conditions is shown in Figure 6. As can be seen, the efficiency of S_2 is better than S_1, which implies that the presence of both metal ions affected the efficiency held considerably and operated cooperatively. According to a study provided by Khademinia et al., cooperative catalysis accelerates some specific chemical transformations.[51] Briefly, cooperation catalytic property among Co^{3+}, Co^{2+}, and Eu^{3+} species is due to the electron transfer by providing the activation energy to transfer valance electron to a higher level. It is found that the optical band gap energies of Eu_2O_3 and Co_3O_4 are 4.4 and 1.96 eV, respectively. However, Eu_2O_3 is a photoluminescent material that has sharp emissions at about 550 and 620 nm that can provide the energy to pump and

excite the electron of Co conduction electron to the higher level and make the electron–cavity pair. So, the catalytic reaction can be performed more efficiently by the cooperation of Eu and Co metal ions.

To assess the capability of the current procedure in the obtaining the final product, as a trial chemical, the present work was compared with some previously reported studies (Table 7). The summarized results clearly revealed that the method suggested in this research could be superior to the reaction time, temperature, and in terms of yield of the target material. In addition to the aformentioned superiorities, the reaction was carried out under mild reaction and solvent-free conditions using an affordable and available catalyst to attain the expected products.

3.7 | Catalyst recyclability

The reusability performance of the catalysts was investigated after multiple runs. The reaction of benzaldehyde, β-naphthol, and malononitrile under modified conditions was regarded as a norm. After each reaction completion, the catalysts were recycled by filtration through rinsing with hot ethanol following by drying. Catalysts were

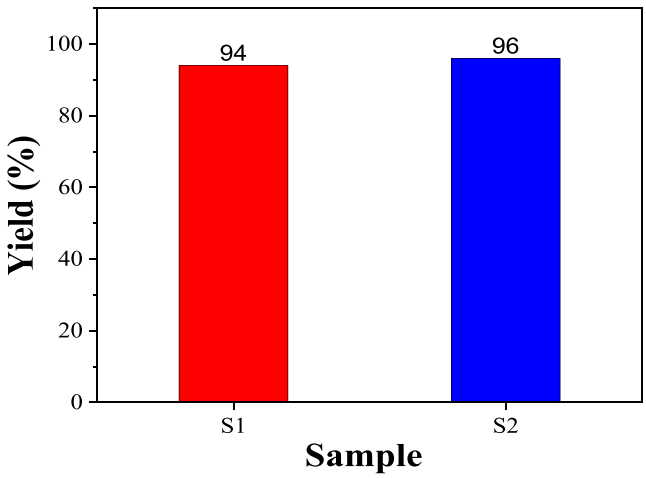

FIGURE 6 Catalytic performance of S_1 and S_2 at the optimum conditions

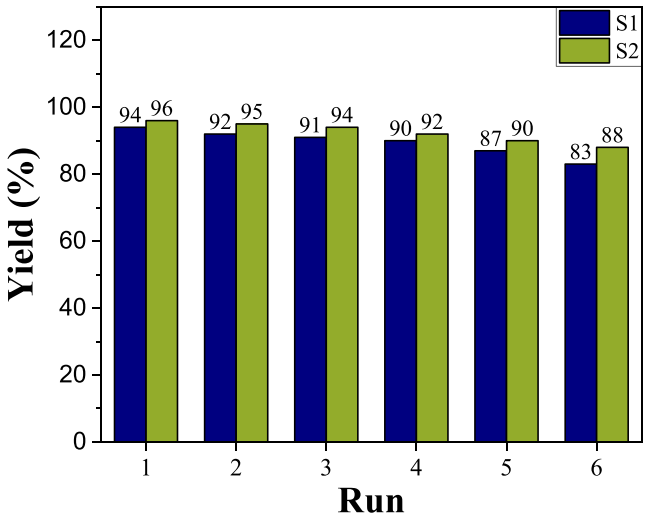

FIGURE 7 Reusability tests for model reaction using (a) S_1 and (b) S_2 as nanocatalysts

TABLE 7 Efficiency comparison of the different catalysts and conditions of previously reported studies with current research

Entry	Catalysts	Reaction condition	Time (min)	Yield (%)	Ref.
1	$FeTiO_3$	MW	9–13	87–94	Taghavi Fardood et al.[52]
2	Water extract of pomegranate peel ash (WEPPA)	MW	4–6	86–90	Hiremath and Kamanna[53]
3	Piperazine	MW	6–8	82–95	Mobinikhaledi et al.[54]
4	1-Butyl-3-methyl imidazolium ([bmim][PF_6])	MW	2 h	70–90	Rao et al.[55]
5	Silica tungstic acid	Solvent-free	1.5–5 h	65–95	Farahi et al.[56]
6	Sodium lauryl sulfate (SLS)	Solvent-free/EtOH	65–220	69–86	Singh et al.[57]
7	MOF-5	Solvent-free	20–45	77–95	Arzehgar et al.[58]
8	Water extract of lemon fruit shell ash (WELFSA)	MW	2–8	84–90	Kantharaju and Khatavi[25]
9	Water extract of banana peel ash (WEB)	MW Grindstone/H_2O	2–8 15–35	72–79	Kantharaju and Khatavi[59]
10	NiO	MW	3	76–99	Neela et al.[60]
11	Co_3O_4/Eu-doped Co_3O_4	MW	4–7	94–99	Present work

Abbreviation: MW, molecular weight.

reused in the next runs under comparable conditions. Figure 7, indicates a sustained activity of the catalysts during six runs without any significant activity loss.

4 | CONCLUSION

The current study reports an ultrasonic-assisted solvothermal procedure for the synthesis of S_1 and S_2 nanomaterials. The XRD analysis revealed that the crystals of the prepared catalysts were spinel cubic with Fd3m space group. FESEM images revealed that doping has a considerable impact on the nanocatalyst morphology. Accordingly, the morphology of the Co_3O_4 changed from agglomerated spherical to nanorods due to the doping Eu^{3+} into the Co_3O_4. The prepared nanocatalysts were also used as heterogeneous catalysts for the synthesis of 2-amino-4*H*-benzochromenes. The prominent conclusion was that the optimum conditions were 30 mg of catalyst and 4- to 7-min duration, and higher efficiency was achieved using S_1 catalyst. The prepared nanocatalyst can be used potentially to synthesize other types of compounds such as benzoxanthenes and benzopyrans either. In addition, the effect of Eu amount on nanocatalyst structure and efficiency can be studied for future investigations.

ACKNOWLEDGMENT

The authors are grateful to Urmia University for supporting this research.

AUTHOR CONTRIBUTIONS

Leila Kafi-Ahmadi: Conceptualization; data curation; investigation; methodology; project administration; supervision; validation. **Ahmad Poursattar Marjani:** Conceptualization; data curation; investigation; methodology; project administration; software; supervision; validation. **Ehsan Nozad:** Data curation; investigation; software; validation.

ORCID

Leila Kafi-Ahmadi https://orcid.org/0000-0001-8947-2706
Ahmad Poursattar Marjani https://orcid.org/0000-0002-5899-4285
Ehsan Nozad https://orcid.org/0000-0002-5608-4923

REFERENCES

[1] A. Kheirollahi, M. Pordeli, M. Safavi, S. Mashkouri, M. R. Naimi-Jamal, S. K. Ardestani, *Naunyn-Schmiedeberg's Arch. Pharmacol.* **2014**, *387*, 1199.
[2] T. H. Afifi, R. M. Okasha, H. E. A. Ahmed, J. Ilas, T. Saleh, A. S. Abd-El-Aziz, *EXCLI J.* **2017**, *16*, 868.
[3] A. Rafinejad, A. Fallah-Tafti, R. Tiwari, A. N. Shirazi, D. Mandal, A. Shafiee, K. Parang, A. Foroumadi, T. Akbarzadeh, *DARU J. Pharm. Sci.* **2012**, *20*, 100.
[4] M. Kidwai, S. Saxena, M. K. R. Khan, S. S. Thukral, *Bioorg. Med. Chem. Lett.* **2005**, *15*, 4295.
[5] X. Y. Meng, H. J. Wang, C. P. Wang, Z. H. Zhang, *Synth. Commun.* **2011**, *41*, 3477.
[6] A. Poursattar Marjani, B. Ebrahimi Saatluo, F. Nouri, *Iran J. Chem. Chem. Eng.* **2018**, *37*, 149.
[7] M. Kargar Karkhah, H. Kefayati, S. Shariati, *Appl. Organomet. Chem.* **2019**, *33*, 5139.
[8] H. Ebrahimiasl, D. Azarifar, *Appl. Organomet. Chem.* **2020**, *34*, 5359.
[9] M. Anvari Gharabaghlou, N. Shadjou, A. Poursattar Marjani, *Appl. Organomet. Chem.* **2020**, *34*, e5868.
[10] A. Mohammadzadeh, A. Poursattar Marjani, A. Zamani, *S. Afr. J. Chem.* **2020**, *73*, 55.
[11] M. Fallah, S. Sohrabnezhad, M. Abedini, *Appl. Organomet. Chem.* **2019**, *33*, e4801.
[12] S. S. Islam, N. Salam, R. A. Molla, S. Riyajuddine, N. Yasmin, D. Das, K. Ghoshe, S. M. Islam, *Mol. Catal.* **2019**, *477*, 110541.
[13] M. Hamza, M. Ayoub, R. B. Shamsuddin, A. Mukhtar, S. Saqib, I. Zahid, M. Ameen, S. Ullah, A. G. Al-Sehemi, M. Ibrahim, *Environ. Technol. Innov.* **2020**, *21*, 101200.
[14] Y. Lv, C. Han, Y. Zhu, T. Zhang, S. Yao, Z. He, L. Dai, L. Wang, *J. Mater. Sci. Technol.* **2021**, *75*, 96.
[15] M. N. Khan, S. Pal, S. Karamthulla, L. H. Choudhury, *RSC Adv.* **2014**, *4*, 3732.
[16] S. K. Kundu, A. Bhaumik, *RSC Adv.* **2015**, *5*, 32730.
[17] H. Kiyani, F. Ghorbani, *Chem. Pap.* **2014**, *68*, 1104.
[18] S. Nagaraju, B. Paplal, K. Sathish, S. Giri, D. Kashinath, *Tetrahedron Lett.* **2017**, *58*, 4200.
[19] I. B. Masesane, S. O. Mihigo, *Synth. Commun.* **2015**, *45*, 1546.
[20] F. K. Behbahani, S. Maryam, *J. Korean Chem. Soc.* **2013**, *57*, 357.
[21] V. A. Osyanin, D. V. Osipov, Y. N. Klimochkin, *Tetrahedron* **2012**, *68*, 5612.
[22] T. S. Jin, J. C. Xiao, S. J. Wang, T. S. Li, *Ultrason. Sonochem.* **2004**, *11*, 393.
[23] A. Maleki, R. Ghalavand, R. F. Haji, *Appl. Organomet. Chem.* **2018**, *32*, e3916.
[24] S. Shinde, S. Damate, S. Morbale, M. Patil, S. S. Patil, *RSC Adv.* **2017**, *7*, 7315.
[25] K. Kantharaju, S. Y. Khatavi, *ChemistrySelect* **2018**, *3*, 5016.
[26] N. V. Shitole, K. F. Shelke, S. A. Sadaphal, B. B. Shingate, M. S. Shingare, *Green Chem. Lett. Rev.* **2010**, *3*, 83.
[27] A. Rezaei, O. Akhavan, E. Hashemi, M. Shamsara, *Chem. Mater.* **2016**, *28*, 3004.
[28] H. Aghadoosi, A. Ramazani, N. Safarvand, Z. Ranjdoost, A. Souldozi, K. Slepokura, T. Lis, *Org. Lett.* **2019**, *21*, 22.
[29] S. R. Bonyad, Z. Mirjafary, H. Saeidian, M. Rouhani, *J. Mol. Struct.* **2019**, *1197*, 164.
[30] Z. Hosseinzadeh, A. Ramazani, H. Ahankar, K. Slepokura, *Silicon* **2019**, *11*, 2169.
[31] S. K. Das, S. Chaterjee, S. Mendal, A. Bhaumik, *Mol. Catal.* **2019**, *475*, 110483.
[32] A. Poursattar Marjani, J. Khalafy, F. Majidi Arlan, E. Eyni, *ARKIVOC* **2019**, *2019*, 1.
[33] A. Nouri, A. Poursattar Marjani, J. Khalafy, *J. Heterocyclic Chem.* **2019**, *56*, 2912.

[34] Z. Hosseinzadeh, N. Razzaghi, A. Ramazani, H. Aghahosseini, A. Ramazani, *Turk. J. Chem.* **2020**, *44*, 194.
[35] J. Khalafy, F. Majidi Arlan, A. Poursattar Marjani, V. Sarchami, *J. Heterocyclic Chem.* **2020**, *57*, 3961.
[36] M. Aslanpanjeh, A. Poursattar Marjani, J. Khalafy, N. Etivand, *Res. Chem. Intermed.* **2020**, *46*, 165.
[37] A. Nouri, A. Poursattar Marjani, J. Khalafy, N. Etivand, *Res. Chem. Intermed.* **2020**, *46*, 3025.
[38] A. Poursattar Marjani, J. Khalafy, P. Eslamipour, M. Ahmadi Sabegh, *Iran J. Chem. Chem. Eng.* **2019**, *38*, 51.
[39] A. Kumar, Y. Kuang, Z. Liang, X. Sun, *Mater. Today Nano.* **2020**, *11*, 100076.
[40] T. Gao, Y. Yin, G. Zhu, Q. Cao, W. Fang, *Catal. Today* **2020**, *355*, 252.
[41] C. Zhao, Y. Tang, C. Yu, X. Tan, M. N. Banis, S. Li, G. Wan, H. Huang, L. Zhang, H. Yang, J. Li, X. Sun, J. Qiu, *Nano Today* **2020**, *34*, 100955.
[42] J. Ma, H. Wei, Y. Liu, X. Ren, Y. Li, F. Wang, X. Han, E. Xu, X. Cao, G. Wang, F. Ren, S. Wei, *Int. J. Hydrogen Energy* **2020**, *45*, 21205.
[43] D. Zagoraios, A. Athanasiadi, I. Kalaitzidou, S. Ntais, A. Katsaounis, A. Caravaca, P. Vernoux, C. G. Vayenas, *Catal. Today* **2020**, *355*, 910.
[44] M. Salehi, R. Abdoos, B. Bahramian, *J. Appl. Chem.* **2018**, *12*, 99.
[45] S. J. Davarpanah, R. Karimian, F. Piri, *J. Appl. Biotechnol. Rep.* **2014**, *1*, 117.
[46] B. M. Abu-Zied, S. A. Soliman, *Catal. Lett.* **2009**, *132*, 299.
[47] M. Ebrahimi, S. Abdolmohammadi, R. Kia-Kojoori, *J. Chin. Chem. Soc.* **2020**, *67*, 1895.
[48] S. Maddila, O. A. Abafe, H. N. Bandaru, S. N. Maddila, P. Lavanya, N. Seshadri, S. B. Jonnalagadda, *Arab. J. Chem.* **2019**, *12*, 3814.
[49] M. Khodajoo, S. Sayyahi, S. J. Saghanezhad, *Russ. J. Gen. Chem.* **2016**, *86*, 1177.
[50] B. Karami, M. Farahi, M. Bazrafshan, S. Khodabakhshi, *S. Afr. J. Chem.* **2014**, *67*, 10.
[51] S. Khademinia, M. Behzad, H. Samari Jahromi, *RSC Adv.* **2015**, *5*, 24313.
[52] S. Taghavi Fardood, A. Ramazani, P. Azimzadeh Asiabi, Y. Bigdeli Fard, B. Ebadzadeha, *Asian J. Green. Chem.* **2017**, *1*, 34.
[53] P. B. Hiremath, K. Kamanna, *Curr. Microw. Chem.* **2019**, *6*, 30.
[54] A. Mobinikhaledi, H. Moghanian, F. Sasani, *Synth. React. Inorganic, Met. Nano-Metal Chem.* **2011**, *41*, 262.
[55] M. S. Rao, B. S. Chhikara, R. Tiwari, A. N. Shirazi, K. Parang, A. Kumara, *Chem.-Biol. Interact.* **2012**, *2*, 362.
[56] M. Farahi, B. Karami, S. Alipour, L. T. Moghadam, *Acta Chim. Slov.* **2014**, *61*, 94.
[57] R. Singh, D. D. Agarwal, M. C. Agarwal, *Inter. J. Innov. Res. Grow.* **2017**, *4*, 100.
[58] Z. Arzehgar, V. Azizkhani, S. Sajjadifar, M. H. Fekri, *Chem. Methodol.* **2019**, *3*, 251.
[59] K. Kantharaju, S. Y. Khatavi, *Asian J. Chem.* **2018**, *30*, 1496.
[60] A. Neela, T. Clarina, V. Rama, *Asian J. Chem.* **2019**, *5*, 1049.

SUPPORTING INFORMATION

Additional supporting information may be found online in the Supporting Information section at the end of this article.

How to cite this article: L. Kafi-Ahmadi, A. Poursattar Marjani, E. Nozad, *Appl Organomet Chem* **2021**, e6271. https://doi.org/10.1002/aoc.6271